Proceedings of the 14th IEEE
International Conference on Nanotechnology
Toronto, Canada, August 18-21, 2014

Tunable and Miniaturized RF Components with Nanocomposite and Nanolayered Dielectrics

P. Markondeya Raj, Parthasarathi Chakraborti, Himani Sharma, KyuHwan Han, Saumya Gandhi,
Srikrishna Sitaraman, Madhavan Swaminathan and Rao Tummala

Packaging Research Center,
Georgia Institute of Technology, Atlanta, GA 30332-0560
Email: raj@ece.gatech.edu

***Abstract*— Nanocomposite and nanolayered dielectrics provide new avenues to enhance the performance of RF and power components. They enable engineering of properties such as permeability, permittivity, frequency- and temperature-stability, and tunability, along with low loss, to miniaturize next-generation multiband RF modules that require higher functional density and improved performance. This paper demonstrates two such advances in nanodielectrics: 1.)Magnetic nanocomposites for miniaturization of antennas, metamaterials and other RF components, 2.)Nanolayered stack dielectrics for tunable RF components with temperature- and frequency-stability and low loss. The materials design, synthesis, processing and characterization to demonstrate the superior properties are presented.**

I. INTRODUCTION

Wireless communication modules are an integral part in all systems and are required to support multiple wireless standards such as Bluetooth, WLAN and GSM. Market trends indicate that in addition to supporting current functionality, future electronic systems need to integrate new applications such as security and healthcare. In order to accommodate such additional functionality, next-generation systems require high-density RF integration that incorporates several frequency bands that are very closely spaced, with improved power efficiency over current modules. These requirements are driving a variety of disruptive component and module packaging technologies with a) 10x increase in active and passive component densities, b.)components with high linearity and quality factor, b) an order of magnitude reduction in form factor, cost and power consumption, and c) higher reliability in spite of increased thermal loads. The primary goal of all the new technologies is to reduce size (area and height), increase performance and reduce cost. The main challenges to system integration and miniaturization arise from the passive components that typically outnumber the active components by more than 10-to-1.

Given the large number of wireless bands in LTE (GSM), a device that can operate in all LTE bands across the world requires a large number of passive components to support all the bands. This causes the cost and size of the system to increase drastically. Alternatively, by integrating tunable components, the number of components is reduced thereby enabling a high-performance world-LTE device in a miniaturized form-factor. To this end, tunable nanolayered dielectrics are gaining importance for tuning filters, matching networks, and other RF circuits.

Current leading-edge RF passives are mostly based on either low-temperature co-fired ceramics (LTCC) or organic substrates. However, their low dielectric permittivity and lack of high-permeability material integration result in larger components and imposes several design constraints for miniaturization and integration. Incorporation of ceramic fillers in polymer matrices is widely pursued to enhance the properties while retaining low-cost and large-area processability with traditional packaging infrastructure. Several advances were made in the ceramic-polymer nanocomposites for high-frequency RF dielectric applications with permittivities that are 3-4X higher than that of the baseline polymer matrix. However, such dielectrics suffer from thermal instabilities and lack of tunability. Similarly, major improvements have not been achieved with magneto-dielectrics because of the inherent limitations in the availability of materials with high frequency-stability and low loss, while retaining the high permeability.

This paper demonstrates metal-polymer nanocomposite and nanolayered dielectric approaches to address the challenges with traditional composite dielectrics. The first part of this paper investigates the frequency-stability of permeability and suppression of magnetic loss in metal-polymer nanocomposites for RF applications. The trade-offs in permeability, frequency stability and loss tangent are described using analytical equations, followed by synthesis and characterization. The second part of the paper describes nanolayered RF dielectrics with self-compensating temperature deviation in the nanolayers, while also allowing tunability.

II. MAGNETIC NANOCOMPOSITE DIELECTRICS

Magnetic nanocomposites provide several advantages for RF applications: a.) low eddy current and domain wall losses from nanoscale particle size; b.) high frequency-stability because of various contributions from magnetic anisotropies that enhance the ferromagnetic resonance frequency (FMR). They also show enhanced permittivity with low loss for further component miniaturization and performance

978-1-4799-5622-7/$31.00 ©2014 IEEE

enhancement. However, they suffer from several limitations which result in suppression of permeability and enhanced damping, leading to high losses over a broad frequency range. The first part of this paper models the effective permeability and frequency stability of the nanocomposites are modeled using simple analytical equations.

Nanocomposite Models:

The permeability variation as a function of metal loading is modeled using the Bruggeman's Effective Medium Theory Model (EMT) [1,2] as shown in Equation 1.

$$c_a \frac{\mu_a - \mu_{eff}}{\mu_a + 2\mu_{eff}} + c_b \frac{\mu_b - \mu_{eff}}{\mu_b + 2\mu_{eff}} = 0 \qquad (1)$$

where μ_a and μ_b refer to the permeabilities of the filler and matrix, c_a and c_b refer to the volume fraction of the filler and matrix, and μ_{eff} is the effective nanocomposite permeability. The nanocomposite permeabilities for various particle permeabilities (assuming the matrix permeability as 1) are shown in Fig. 1

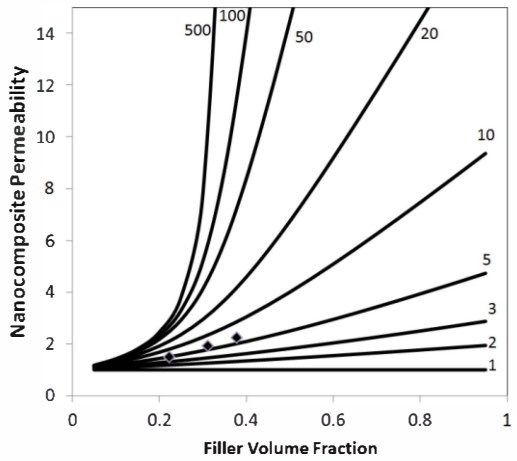

Fig. 1: Nanocomposite permeability plots assuming various particle permeabilities. The measured values coincide with the curve having a filler permeability of 5.

The losses are attributed to various sources. For large metal particles, eddy current losses significantly contribute to the total losses. Hysteresis losses arise from the coercivity. When the particle size exceeds a critical dimension, domains are formed within the particle. The domain wall resonance also contributes to losses. Losses are further increased as the frequency reaches the ferromagnetic resonance (FMR).

The eddy current losses in metal-nanocomposites are a strong function of the particle size, particle conductivity and the frequency. The frequency (F_{EC}) above which the eddy current losses dominate is estimated using the equation [3]:

$$F_{EC} = \frac{4\rho}{\pi\mu_o(1+X)D^2} \qquad (2)$$

where $\boldsymbol{\rho}$ is the conductivity and $\boldsymbol{X}$ is the magnetic susceptibility. Estimated F_{EC} for 25 nm particles is much more than 10 GHz, again indicating that eddy currents are not dominant. Previous studies [1] also indicate that particles with size in the 10-100 nm range do not show substantial eddy current losses even in several GHz range.

The losses from domain walls occur when multiple domains are present within the particles, and are usually dominant at 1-250 MHz frequencies for microsized ferrites and metallic nanoparticles [4, 5]. The frequency (F_{DW}) where the domain wall losses dominate is given as [3]:

$$F_{DW} = \sqrt{\frac{2\delta(n+1)}{3\pi\,(1+X)D}}\ \frac{\gamma J_s}{2\pi\mu_o} \qquad (3)$$

where δ is the domain wall thickness, $\boldsymbol{\gamma}$ is the gyromagnetic ratio, D_d is the domain spacing or domain size, n is the number of domains in a particle with diameter D, μ_o is the permeability of free space, $\boldsymbol{X}$ is the susceptibility of the material, J_s is the saturation polarization.

The domain wall thickness is dependent on the exchange constant (A) and the magnetic anisotropy energy density (K). The domain size varies with the particle dimensions. In case of larger microscale particles, domain wall resonances lead to magnetic losses at lower frequencies. Finer particles show domain wall resonance at higher frequencies, while these losses are absent in single-domain nanoparticles [6,7]. The sum of critical domain size and domain wall thickness for cobalt exceeds 25 nm, suggesting that these particles are single-domain and do not contain any domain walls.

The maximum operation frequency of the material is determined by the FMR when eddy current, domain wall and hysteresis losses are eliminated. The FMR is related to the effective field anisotropy. In simpler terms, the FMR frequency is written as [8]:

$$F_{FMR} = \frac{\gamma}{2\pi} H_{Eff} \qquad (4)$$

Nanoscale particles show enhanced field anisotropy from the single domains that are present within the particle and the ferromagnetic-antiferromagnetic coupling at the cobalt-cobalt oxide interfaces where cobalt forms the ferromagnetic core and the oxide acts as the antiferromagnetic shell [9, 10]. All these factors contribute to high field anisotropy and coercivity, which suppresses the permeability and enhances the frequency stability.

The field anisotropy (H_{eff}) is related to the anisotropy energy density (K) as [11]:

$$H_{Eff} = \frac{4|K|}{3\mu_o M_s} \qquad (5)$$

The anisotropy energy is attributed to the bulk and surface contributions [10]:

$$K = K_{bulk} + \frac{6\,K_{surface}}{D} \qquad (6)$$

These equations provide a simple theoretical basis to estimate permeability and FMR as a function of particle size and filler loading.

The magnetic losses increase as the frequency reaches the FMR. However, isotropic nanocomposites show broad FMR behavior. Therefore, the losses are higher even at lower frequencies. Anisotropic one-dimensional nanostructures based on nickel or cobalt nanowires or filaments have been modeled, designed and fabricated to overcome the limitations of isotropic nanocomposites [12,13]. The FMR increases with aspect ratio, as shown in a theoretical analysis by Nam et al. [12]. For composites consisting of nanowires with both shape and crystal anisotropy, the FMR is proportional to the net field anisotropy, which also includes the dipolar interactions. When the magnetocrystalline axis is parallel to the wire axis, FMR is as written as [13]:

$$\frac{\omega_{FMR}}{\gamma} = H + 2\pi M_s - 6\mu M_s P + H_u \quad (7)$$

H is the effective resonance field, $2\pi M_s$ is the shape anisotropy, $-6\pi M_s P$ refers to the dipolar interaction, P is the volume fraction, H_u is the crystal anisotropy.

Synthesis and material characterization:

Cobalt nanoparticles (oxide passivation, 25-50 nm diameter) were first milled in a solvent, and then milled with the epoxy monomer solution to make the nanocomposite slurry. The slurry was dried in an oven and the resultant dry powders were pressed into toroids. The metal-insulator volume ratio was varied from 30:70 to 70:30.

The material characteristics were investigated first to confirm the nanostructure. The particle size, shape and crystallinity were characterized through XRD and TEM. The chemical composition was analyzed through EDS (Energy Dispersive Spectroscopy). B-H loops were obtained with a vibration sample magnetometer (VSM, Lakeshore 736 Series, Westerville, OH).

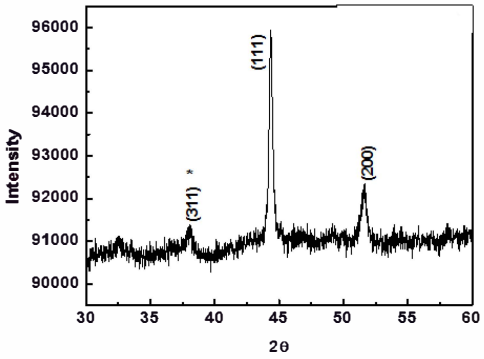

Fig. 2: XRD spectrum of cobalt-polymer nanocomposites.

The XRD spectrum of cobalt-polymer nanocomposites is shown in Fig. 2, which indicates an average crystallite size of ~31 nm for cobalt particles. The peaks matched with (111), (200) and (220) planes of face-centered-cubic (fcc) metallic cobalt. A weak peak corresponding of cobalt oxide at 38^o indicate a thin oxide layer on the metal core. The XRD grain size measurements are consistent with the TEM study shown in Fig. 3.

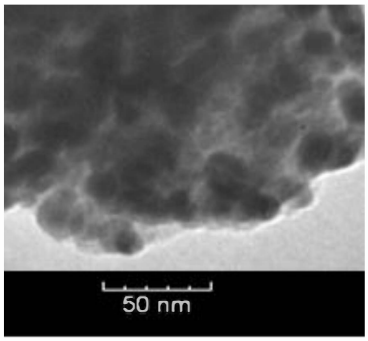

Fig. 3: TEM of cobalt-polymer nanocomposites.

A coercivity of ~800 Oe and Ms of 70 emu/gm was measured from the VSM measurements, as shown in Fig. 4. The theoretical Ms of a nanocomposite with 90 wt.% metal is approximately 144 emu/gm. This indicates that approximately 50 wt.% of the powder weight is converted to cobalt oxide that does not contribute to the Ms. The cobalt oxide shell provide several benefits by acting as an insulating passivation that prevents eddy current losses.

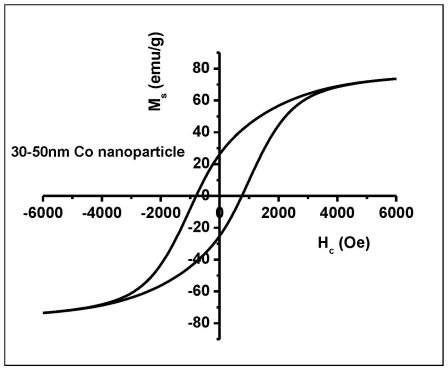

Fig. 4: VSM measurements of hysteresis curve for cobalt-polymer nanocomposites.

Measurements up to 1000 MHz were performed with an impedance analyzer (Agilent 4291B Impedance Analyzer). Cavity perturbation technology (CPT) is a well-known method for measuring electromagnetic properties of materials above 1000 MHz. This technique is applied to characterize the nanocomposite materials at GHz frequencies. Cavities for CPT were implemented by substrate integrated waveguide (SIW) technology described elsewhere [14].

Based on effective medium theory (EMT) model, best fit for the measured properties was obtained when the particle permeability is ~5-6, as shown in Fig. 1. This corresponds to a field anisotropy of 3300 Oe, from Equation (4). The corresponding K is then calculated as 3.6×10^5 J/m^3, from Equation (5). The intrinsic permeability of nanoparticles is much lower than that for the bulk because of the demagnetization associated with size and shape. The effective field anisotropy is further enhanced in nanoparticles because of surface effects. However, the higher field anisotropy improves the frequency-stability in

magnetic nanocomposites to ~1 GHz, as seen from the high-frequency characterization results in Fig. 5. The characterization results indicate that isotropic nanocomposites enable permeability stability till 1 GHz. The permeability spectrum of anisotropic nanowire structures with improved frequency stability and low loss, reported by Kou et al., [15] are superimposed on the same graph. The anisotropic structures show enhanced FMR and suppressed FMR broadening compared to the isotropic composites. The results indicate that isotropic nanoparticle composites with simpler processing are suitable at frequencies below 1 GHz while anisotropic structures with more processing complexity are needed at higher frequencies.

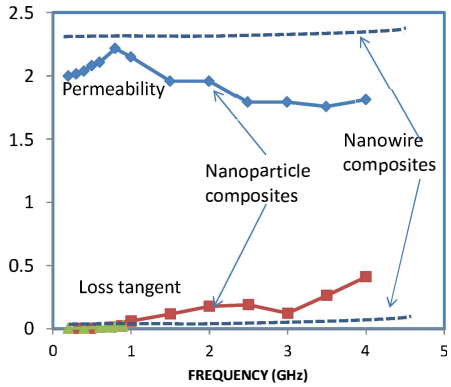

Fig. 5. Extracted nanocomposite properties by combining impedance analyzer and SIW techniques. The properties of nanowire composites [15] are also superimposed on the graph.

III. TUNABLE NANOLAYERED DIELECTRICS

Tunable nanolayered dielectrics are becoming important for tuning filters, matching networks, antennas and other RF circuits. Perovskite films show tunability because the ionic displacement, which leads to dipolar polarization and high permittivity, saturates with increasing electric fields. However, they show high dielectric losses and instability with temperature. Certain other perovskites such as strontium titanate, barium strontium titanate with high Sr content, and calcium titanate are incipient ferroelectrics, where the permittivity varies with temperature in accordance with Curie-Weiss law, but the materials do not undergo paraelectric-to-ferroelectric transition [16]. In normal operating conditions, these films show negative TCC but with low loss, while retaining tunability.

Fig. 6: Nanolayered stack-dielectrics.

Modeling of layered dielectrics: Nanolayered dielectrics with self-compensating superparaelectric-paraelectric thin-film stacks can achieve simultaneous low TCC, low loss and tunability. The capacitance of the layered dielectric structure is written as:

$$\frac{d}{\varepsilon} = \frac{d_1}{\varepsilon_1} + \frac{d_2}{\varepsilon_2} \qquad (8)$$

Analytical models (Equations 8-9) for zero-TCC and tunability in such nanolayered stack are derived as:

$$\frac{d_1}{d_2} = \frac{-\varepsilon_1}{\varepsilon_2}\frac{TC\varepsilon_2}{TC\varepsilon_1} = \frac{\varepsilon_1}{\varepsilon_2}\frac{1}{\propto} \quad \text{where} \quad \alpha = \frac{-TC\varepsilon_1}{TC\varepsilon_2} \qquad (9)$$

These models suggest that a nanolayered dielectric (schematically illustrated in Fig. 6) of incipient ferroelectric (for example, strontium titanate with negative TCε of -2000 ppm/°C) and a nanoscale paraelectric (alumina with a positive TCε of ~100 ppm/°C) is expected to result in a low TCC and low loss because of its internal compensation. Assuming that the TCC does not change with voltage, further analysis of the stack-dielectric also indicates that the tunability of the stack is same as that of Layer 1. In other words, the net tunability is same even though one of the layers is not tunable.

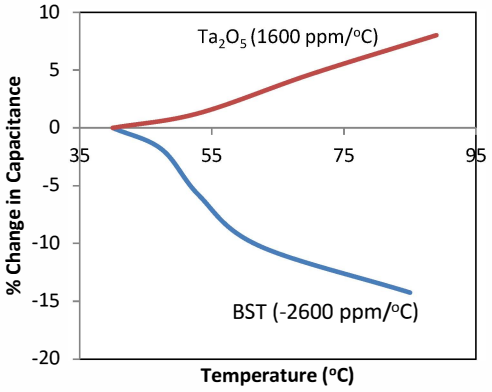

Fig. 7: TCC measurements on individual layers.

Synthesis and Characterization: Barium strontium titanate was RF-sputtered as thin dielectric layers on nickel electrodes deposited on silicon substrates. The RF plasma was powered at a 100 W with an O_2:Ar ratio of 60 sccm : 40 sccm. The films were annealed in Ar at 650 °C to achieve complete crystallanity. A ramp of 5 °C/min was used up to 650 °C and then the films were kept at that temperature for 30 min. The films were characterized with gold top electrodes evaporated through a shadow mask. They showed a capacitance density of 3 nF/mm^2, loss of 0.01 and TCC of 2600 ppm/°C. Based on the film thickness of 200 nm, the permittivity is estimated as ~68. Similarly, tantalum oxide dielectrics were processed from anodization of sputtered tantalum in a phosphoric acid solution. The tantalum oxide dielectrics showed a capacitance density of 1.2 nF/mm^2 (corresponding to a permittivity of 23), loss of 0.01 and TCC of 1600 ppm/°C. The TCC measurements for each of the layers are shown in Fig. 7. The negative and positive TCC

for these two dielectrics provide opportunities for internal compensation in a stack-dielectric as seen in the figure. Based on Equation (8), near-zero TCC will be achieved when the ratio of thickness of strontium titanate and tantalum oxide is ~1.8.

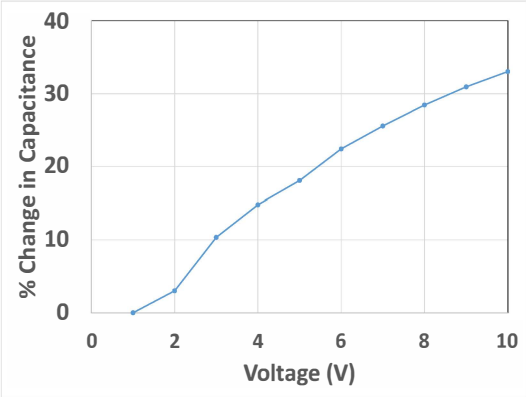

Fig. 8: Tunability measurements from the BST film.

The tunability of the dielectric, which also approximately corresponds to that of the stack, is shown in Fig. 8. The tunability is significant but can be further improved with more stable oxide electrodes instead of nickel and optimized annealing conditions. The results conceptually illustrate that tunable and low TCC dielectrics with low loss can be achieved with the nanolayered stack-dielectric approach.

IV. SUMMARY

Two classes of RF nanodielectrics, viz., metal-polymer nanocomposites and nanolayered dielectrics, and their applications for advanced RF component packaging are demonstrated. Modeling for permeability and frequency-stability of magnetic nanocomposite dielectrics for applications such as antennas and metamaterials, and synthesis and characterization, is described in the first paper of the paper. Tunable high-permittivity nanolayered dielectrics with simultaneous reduction in loss and temperature-instabilities are described in the second part of the paper.

V. REFERENCES

1. Ramprasad R, Zurcher P, Petras M, Miller M, and Renaud P, Fundamental limits of soft magnetic particle composites for high-frequency applications, Phys. Stat. Sol., (2002), 233, No. 1: 31–38.

2. Youngs IJ, Bowler N, Lymer KP and Hussain S, Dielectric relaxation in metal-coated particles: the dramatic role of nanoscale coatings. J. Phys. D: Appl. Phys 2005; 38:188–201.

3. Mazaleyrat F, Varga LK, Ferromagnetic nanocomposites, J. Magn. Magn. Mater 2000; 215-216: 253-259.

4. Wu MZ, Zhang YD, Hui S, Xiao TD, Ge SH, Hines HA, Budnick JI, Taylor GW, Microwave magnetic properties of Co50/(SiO_2)50 nanoparticles. Appl. Phys. Lett (2002), 80: 4404-4406.

5. Abshinova MA, Lopatin AV, Kazantseva NE, Vilcakova J, Saha P, Correlation between the microstructure and the electromagnetic properties of carbonyl iron filled polymer composites, Composites: Part A 38 (2007) 2471–2485.

6. Tang NJ, Zhong W, Liu W, Jiang HY, Wu XL, Du YW, Synthesis and complex permeability of Ni/SiO_2 nanocomposites, Nanotechnology 2004; 15:1756–1758.

7. Lu X, Liang G, Sun Q, Yang C, The influence of silica matrix on the crystal structure and high frequency performance of cobalt nanoparticles, J. Solid State Chem (2010), 183: 1555-1560.

8. Lu B, Dong XL, Huang H, Zhang XF, Zhu XG, Lei JP, Sun JP, Microwave absorption properties of the core/shell-type iron and nickel nanoparticles. J. Mag. Mag. Mater (2008), 320:1106-1111.

9. A. E. Berkowitz and K. Takano, Exchange anisotropy – A review, Journal of Magnetism and Magnetic Materials, (1999), 200: 552-570.

10. Perzynski R and Raikher YL, Surface effects in magnetic nanoparticles, Edited by D. A. Fiorani (Nanostructured Science and Technology Series, Ottawa, Canada), (2005).

11. Zhang XF, Dong XL, Huang H, Liu YY, Wang WN, Zhu XG, Lu B, Lei LP, and C. G. Lee CG, Microwave absorption properties of the carbon-coated nickel nanocapsules. App. Phys. Lett 2006; 89: 053115.

12. Nam B, Choa YH, Oh ST, Lee SK, Kim KH, Broadband RF Noise Suppression by Magnetic Nanowire-Fill Composite Films. Magnetics, IEEE Transactions on 2009, 45(6):2777-2780.

13. Darques M, Spiegel J, De la Torre Medina J, Huynen I, Piraux L, Ferromagnetic nanowire-loaded membranes for microwave electronics. Journal of magnetism and magnetic materials 2009, 321(14):2055-2065.

14. Han K, Swaminathan M, Sharma H, Raj PM, Tummala R, and Nair V, Magnetodielectric characterization and antenna design, Proceedings, Electronic Components and Technology Conference, 2014, 782-788.

15. Kou X, Fan X, Zhu H, Cao R, Xiao JQ: Microwave Permeability and Tunable Ferromagnetic Resonance in Cobalt Nanowire Arrays. Magnetics, IEEE Transactions on 2010, 46(5):1143-1146.

16. Reaney IM, Wise P, Ubic R, Breeze J, Alfred NM, Iddles D, Cannell D and Price T, On the temperature coefficient of resonant frequency in microwave dielectrics, Phil. Mag A, (2001), 81, 2:501-510.